

# Nonisothermal Crystallization Kinetics of Polytetrafluoroethylene/Solid Glass Microsphere Composites

Zhi-Chao Wang,<sup>1</sup> Kai-Chang Kou,<sup>1</sup> Min Chao,<sup>1</sup> Hui Bi,<sup>1</sup> Lu-Ke Yan<sup>2</sup>

<sup>1</sup>School of Science, Northwestern Polytechnical University, Xi'an 710129, China

<sup>2</sup>School of Materials Science and Engineering, Chang'an University, Xi'an 710064, China

Received 7 December 2008; accepted 11 December 2009

DOI 10.1002/app.31933

Published online 26 March 2010 in Wiley InterScience (www.interscience.wiley.com).

**ABSTRACT:** The nonisothermal crystallization behavior and kinetics of polytetrafluoroethylene (PTFE) and PTFE/solid glass microsphere (SGM) composites were investigated with differential scanning calorimetry at various cooling rates ( $\Phi$ 's). Three methods, namely, the Jeziorny, Ozawa and Mo methods, were used to describe the nonisothermal crystallization process. The results show that the peak temperature, crystallinity ( $X_c$ ), and crystallization half-time were strongly dependent on the content of SGMs and  $\Phi$ . The SGMs in the PTFE/SGM composites exhibited a higher nucleation activity. The nonisothermal crystallization kinetics of PTFE and the PTFE/SGM composites was ana-

lyzed successfully with the Jeziorny and Mo methods; however, the Ozawa equation was invalid for the nonisothermal crystallization process. The crystallization activation energy determined with the Kissinger equation was remarkably lower when a small amount of SGMs (5%) was added and then gradually increased and finally became slightly lower than that of pure PTFE as the content of SGMs increased up to 25% in the composites. © 2010 Wiley Periodicals, Inc. *J Appl Polym Sci* 117: 1218–1226, 2010

**Key words:** composites; differential scanning calorimetry (DSC); polytetrafluoroethylene (PTFE)

## INTRODUCTION

Polytetrafluoroethylene (PTFE) resins have been widely applied in many fields because of their notable properties, such as high thermal stability, unusual toughness at low temperatures, and high resistance to chemical attack.<sup>1,2</sup> However, their bad creep resistance has greatly hampered their further application in the field of aerospace engineering.<sup>3</sup> Therefore, many efforts have been made to improve this by the addition of various fillers to PTFE to overcome these limitations.<sup>4–6</sup>

It is well known that there are strong dependences of the physical and mechanical properties of crystalline polymers on the crystalline structure and crystallinity ( $X_c$ ). The rapid crystallization of PTFE makes it difficult to observe the isothermal crystallization process. Moreover, real industrial processes generally proceed under nonisothermal conditions; thus, the analysis of nonisothermal crystallization kinetics is of great significance. Recently, a large

amount of work concerning the crystallization behavior of PTFE and filled PTFE composites has been done.<sup>7–9</sup> Seo<sup>10</sup> reported on the crystallization kinetics of PTFE under nonisothermal conditions; this study indicated the formation of one-dimensional crystallites (fibrillar type) after thermal nucleation or two-dimensional crystallites (discs) after athermal nucleation. Wang et al.<sup>11</sup> investigated the isothermal and nonisothermal crystallization kinetics of PTFE and the effects of glass fibers on the crystallization behavior of PTFE. They confirmed that PTFE crystals grow one dimensionally and that glass fibers did not obviously affect the crystallization of the PTFE matrix. Kostov et al.<sup>12</sup> studied the thermophysics and crystallization kinetics of polymerization-filled PTFE with  $\text{CaCO}_3$ , and the results reveal that secondary crystallization was not observed in PTFE. However, systematic approaches to the nonisothermal crystallization kinetics of filled PTFE composites, especially to that of PTFE/solid glass microsphere (SGM) composites, have rarely been reported.

In this study, we focused on the influences of SGMs and the cooling rates ( $\Phi$ 's) on the nonisothermal crystallization behavior of PTFE. The experimental data obtained from differential scanning calorimetry (DSC) were thoroughly analyzed on the bases of the Jeziorny, Ozawa and Mo methods. Moreover, the crystallization activation energy ( $\Delta E$ ) was also

Correspondence to: K.-C. Kou (wzc\_gtt@yahoo.com.cn).

Contract grant sponsor: Graduate Starting Seed of Northwestern Polytechnical University; contract grant number: Z200869.

determined with the Kissinger equation to better understand the crystallization behavior of PTFE.

## EXPERIMENTAL

### Materials and sample preparation

PTFE powder was supplied by Jinan 3F Fluoro-Chemical Co., Ltd. (Jinan, China), and SGM was obtained commercially from Qinhuangdao Qinhuang Glass Microsphere Co., Ltd. (Qinhuangdao, China). SGM was introduced into the PTFE matrix in concentrations of 0, 5, 15, and 25%, and the corresponding composites were denoted as P-0, P-5, P-15, and P-25, respectively. The PTFE/SGM composites were prepared as follows. First, the mixing of PTFE and SGM was performed in the presence of acetone. After mixing, acetone was volatilized, and then, the leftovers were dried. Second, the dried powders were molded at a relatively high compressive stress to produce a preform. The preform was heated above the melting

point, maintained for 2 h to allow the particles to coalesce completely, and then cooled to 200°C. Finally, the posttreatment of the resulting substance was carried out at a given temperature and pressure.

### Nonisothermal DSC analysis

The DSC analysis of PTFE and the PTFE/SGM composites was performed on a Q1000DSC Thermoanalyzer System (TA Instruments, New Castle, DE) under a nitrogen flow. Samples weighing between 5 and 10 mg were heated from room temperature to 360°C at a high heating rate and kept for 5 min at this temperature to remove their thermal history. The melt was then cooled to 260°C at desired  $\Phi$ 's of 5, 10, 20, and 40°C/min, respectively. We then observed the subsequent melting behavior by reheating the samples at a heating rate of 20°C/min to 360°C. Both the crystallization exotherms and subsequent melting endotherms were recorded for further analysis.

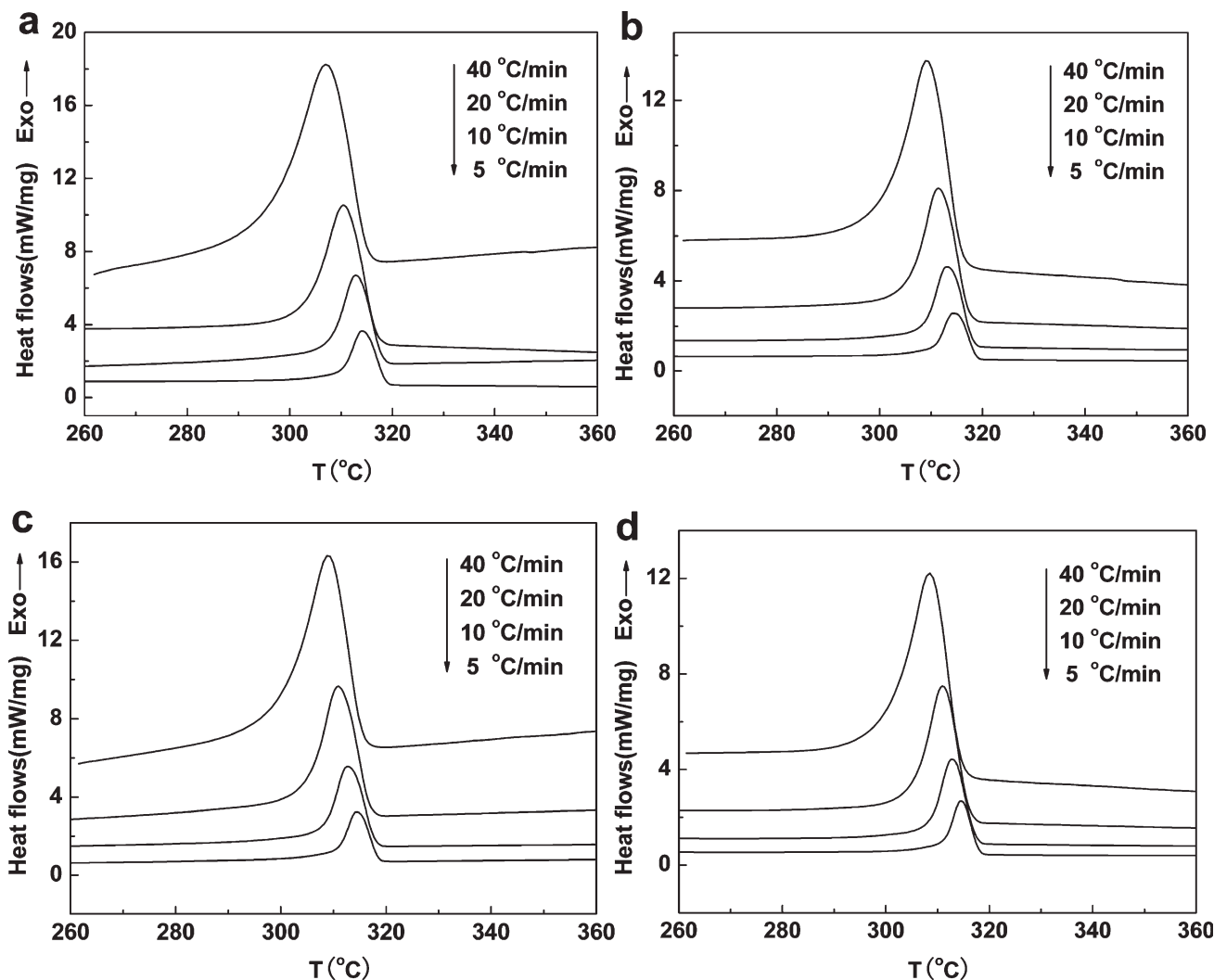


Figure 1 Nonisothermal crystallization exotherms for (a) P-0, (b) P-5, (c) P-15, and (d) P-25 at various  $\Phi$ 's.

TABLE I  
Nonisothermal Crystallization Kinetic Parameters of PTFE and the PTFE/SGM Composites

No.	$\Phi$ (°C/min)	$T_o$ (°C)	$T_p$ (°C)	$D$ (°C)	$\Delta H_m$ (J/g)	$X_c$ (%)	$\Delta E$ (kJ/mol)
P-0	5	318.7	314.0	8.6	14.22	20.6	293.1
	10	318.0	312.9	10.1	13.11	19.0	
	20	316.9	310.3	13.4	12.21	17.7	
	40	315.1	307.0	16.9	10.18	14.8	
P-5	5	318.8	314.3	8.2	9.947	15.2	232.1
	10	318.1	313.2	9.4	9.353	14.3	
	20	317.2	311.5	11.5	8.566	13.1	
	40	315.9	308.9	14.2	7.849	12.0	
P-15	5	318.4	314.3	7.6	11.26	19.2	251.4
	10	317.9	312.8	9.5	10.67	18.2	
	20	316.9	310.9	11.7	9.784	16.7	
	40	315.5	308.7	14.0	8.535	14.6	
P-25	5	317.9	314.5	6.7	8.777	17.0	283.5
	10	317.3	312.9	8.7	8.433	16.3	
	20	316.1	310.9	10.8	7.648	14.8	
	40	314.5	308.5	13.4	6.795	13.1	

## RESULTS AND DISCUSSION

### Nonisothermal crystallization behavior

Figure 1 shows the nonisothermal crystallization exotherms of P-0, P-5, P-15, and P-25 for various

$\Phi$ 's, ranging from 5 to 40°C/min. Clearly, the exothermic peaks became broader and shifted to lower temperatures as  $\Phi$  increased. Thus, crystallization performed at lower temperatures with faster  $\Phi$ 's.

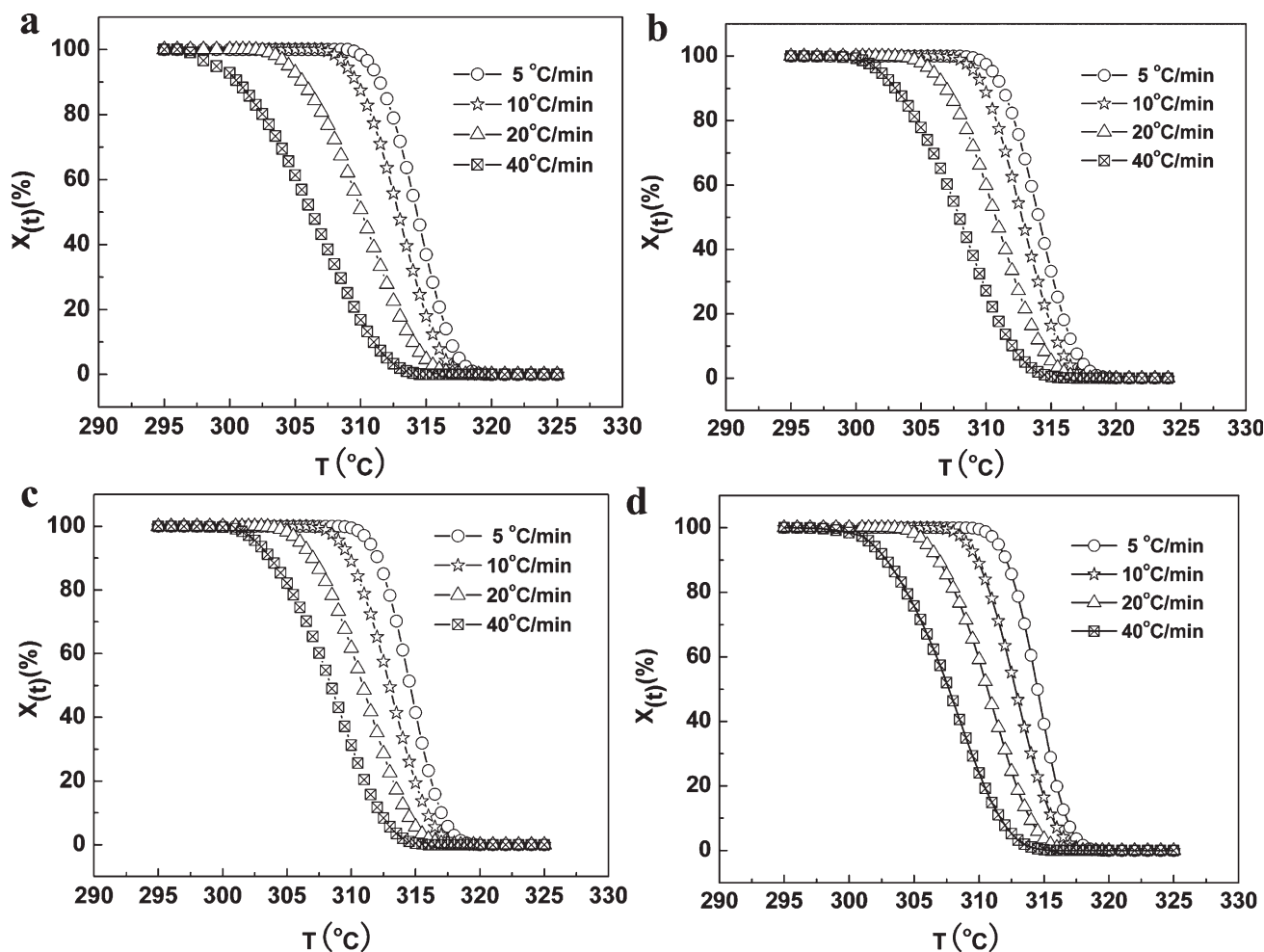


Figure 2 Plots of  $X_c$  as a function of temperature for (a) P-0, (b) P-5, (c) P-15, and (d) P-25 at various  $\Phi$ 's.

For the PTFE/SGM composites,  $X_c$  was calculated as<sup>13</sup>

$$X_c = \Delta H_m / (\Delta H_m^o \alpha) \quad (1)$$

where  $\alpha$  is the mass fraction of PTFE in the PTFE/SGM composites,  $\Delta H_m$  is the melting enthalpy of PTFE, and  $\Delta H_m^o$  represents the melting enthalpy when  $X_c$  is 100%, with a value of 69 J/g.

Some parameters, including the initial crystallization temperature ( $T_o$ ); peak temperature ( $T_p$ ); *crystallinity temperature scale*, defined as the difference value between the onset and end crystallinity temperatures ( $D$ );  $\Delta H_m$ ; and  $X_c$ ; are summarized in Table I.  $X_c$  decreased with increasing  $\Phi$ . At lower  $\Phi$ 's, the molecular segments of PTFE were actively mobile. As  $\Phi$  increased, the activity of the molecular segments decreased, and it was difficult for the molecular segments to arrange into a crystal lattice. As a result, the degree of imperfection of the crystal increased.

To obtain the kinetic information, the experimental data shown in Figure 1 were converted to the rela-

tive degree of crystallinity function of temperature [ $X(t)$ ], which was formulated as<sup>14</sup>

$$X(t) = \int_{T_o}^T \frac{dH_c(T)}{dT} dT \bigg/ \int_{T_o}^{T_\infty} \frac{dH_c(T)}{dT} dT \quad (2)$$

where  $T_o$  and  $T_\infty$  denote the onset and end crystallinity temperatures, respectively, and  $dH_c/dT$  is the crystallization heat flow rate. Plots of  $X(t)$  as a function of the temperature ( $T$ ) for all samples at various  $\Phi$ 's are depicted as in Figure 2. In the nonisothermal crystallization process, when the assumption that the samples experienced the same thermal history as designated by the DSC furnace was valid, the temperature could be converted to the corresponding time ( $t$ ) with the following equation:

$$t = (T_o - T)/\Phi \quad (3)$$

Thereby, Figure 2 with the  $x$  axis in the temperature scale was converted into Figure 3 with the  $x$  axis in the time scale. All of the curves in Figure 3 have a similar sigmoid shape. It was inferred that

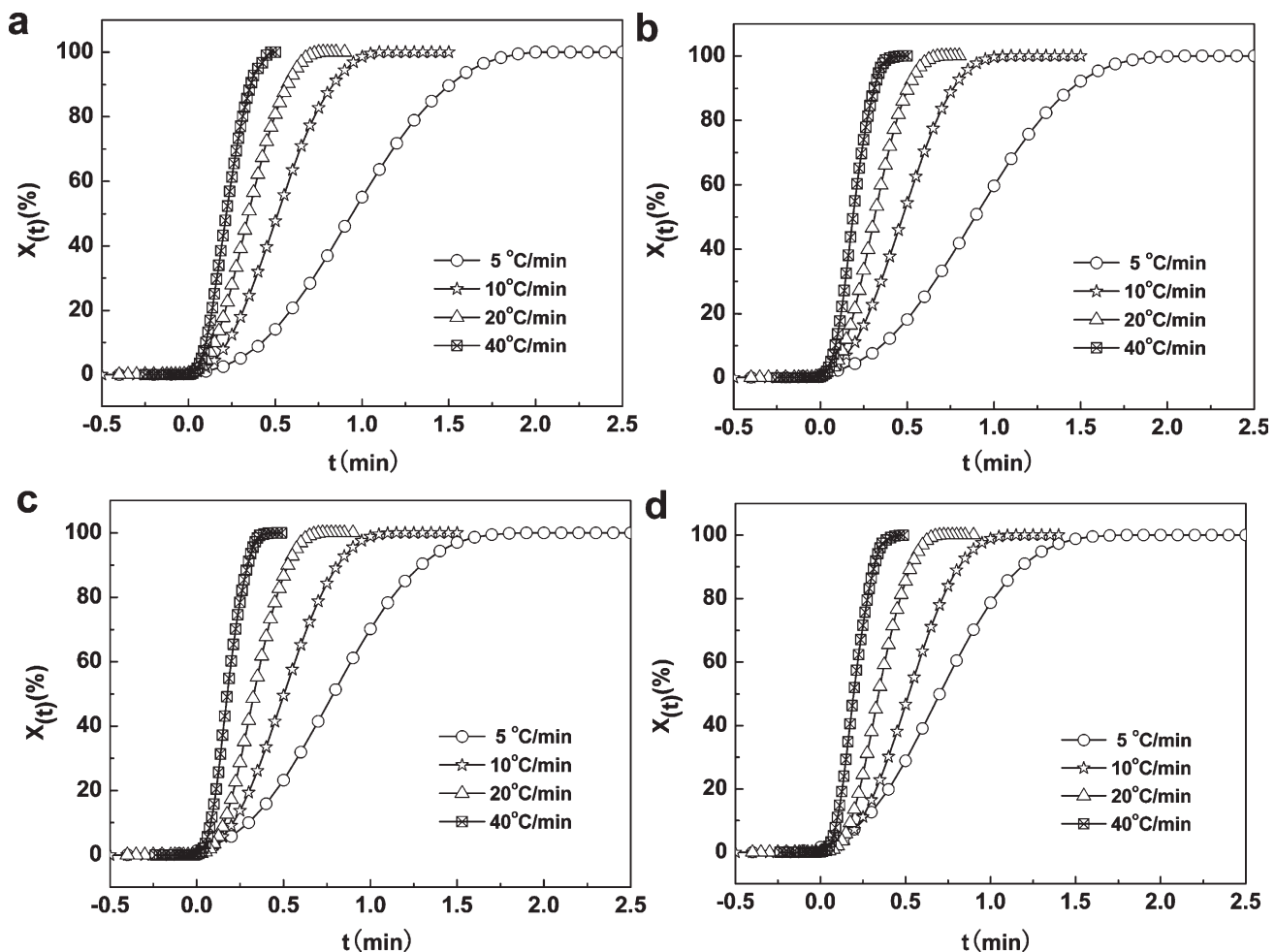


Figure 3 Plots of relative  $X_c$  as a function of crystallinity time for (a) P-0, (b) P-5, (c) P-15, and (d) P-25 at various  $\Phi$ 's.

only the retardation or acceleration effect of  $\Phi$ 's on the crystallization was observed.<sup>15</sup>

### Nonisothermal crystallization kinetics

Various models have been proposed for analyzing the nonisothermal crystallization behavior of polymers. The most commonly used ones are the Ozawa method,<sup>16</sup> Ziabicki method,<sup>17</sup> Jeziorny method,<sup>18</sup> Gupta method,<sup>19</sup> and Mo method.<sup>20</sup> In this study, we applied the Jeziorny, Ozawa, and Mo methods to the analysis.

#### Jeziorny method

The isothermal crystallization kinetics of a polymer is generally studied by the Avrami method.<sup>21,22</sup> Jeziorny<sup>18</sup> considered the nonisothermal crystallization process as an isothermal crystallization process by assuming that the crystallization temperature was a constant. The Avrami equation was defined as

$$\log\{-\ln[1 - X(t)]\} = \log Z + n \log t \quad (4)$$

where  $n$  is the Avrami exponent and  $Z$  represents the Avrami crystallization rate constant; both of them are constants specific to a given crystalline morphology and type of nucleation for a particular crystallization condition. With the nonisothermal character of the process investigated considered, the value of  $Z$  should be appropriately corrected. The final form is given as follows:

$$\log Z_c = \frac{\log Z}{\Phi} \quad (5)$$

where  $Z_c$  is the modified crystallization rate constant.

Plots of  $\log\{-\ln[1 - X(t)]\}$  versus  $\log t$  at various  $\Phi$ 's are represented in Figure 4. The good linearity demonstrated that this method satisfactorily described the nonisothermal crystallization process of PTFE and the PTFE/SGM composites. The values of  $n$ ,  $Z$ ,  $Z_c$ , crystallization half-time ( $t_{1/2}$ ), and the reciprocal of  $t_{1/2}$  ( $\tau_{1/2}$ ) are listed in Table II. It is clear from Figure 4 that the slopes were close and all  $n$  values ranged from 2 to 2.7, which implied that the SGMs had less effect on the

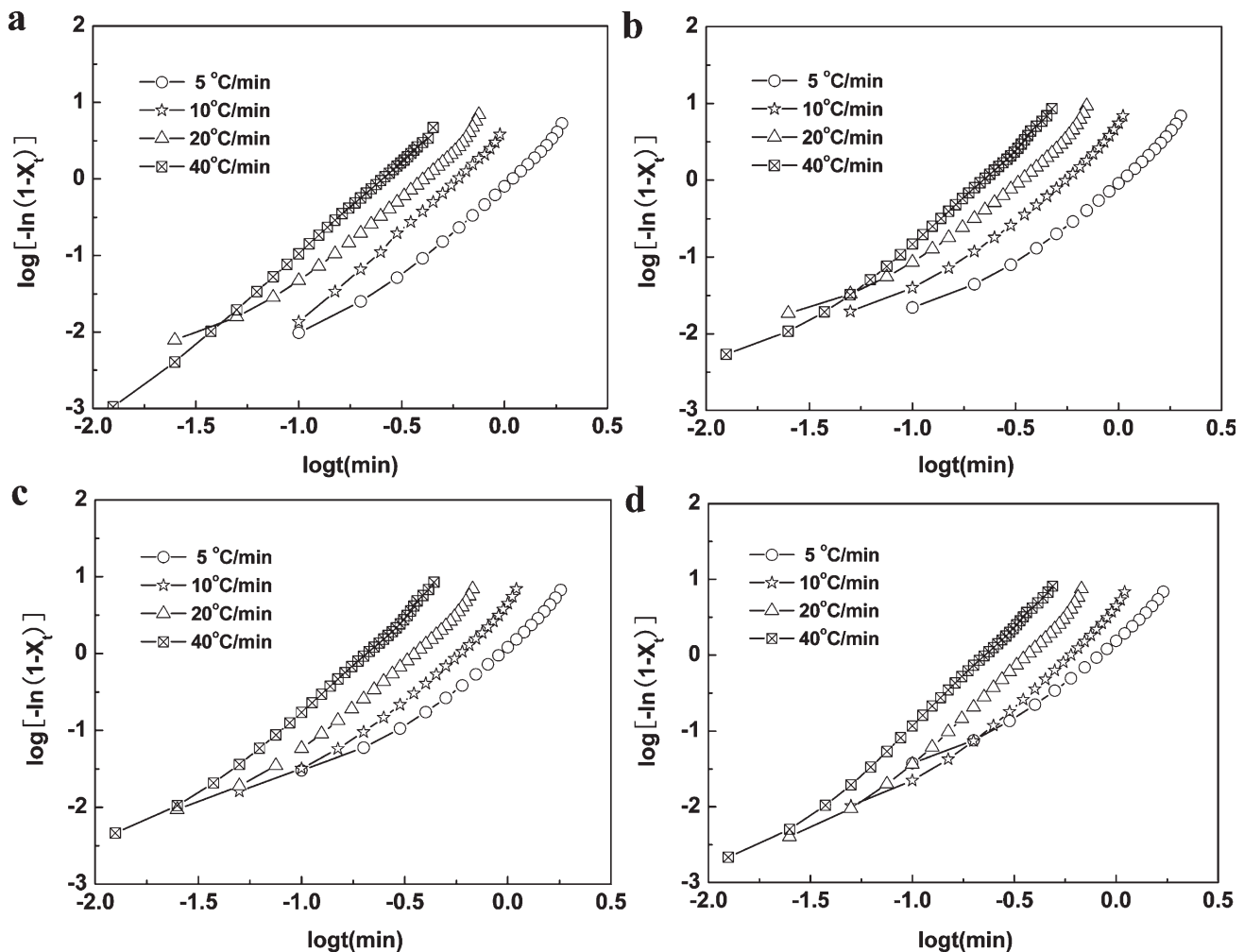


Figure 4 Plots of  $\log\{-\ln[1 - X(t)]\}$  versus  $\log t$  for (a) P-0, (b) P-5, (c) P-15, and (d) P-25.

TABLE II  
Parameter Values of Nonisothermal Crystallization Obtained with the Jeziorny Equation and  $\Delta E$  of PTFE and the PTFE/SGM Composites

No.	$\Phi$ ( $^{\circ}\text{C}/\text{min}$ )	$n$	$Z$	$Z_c$	$t_{1/2}$ (min)	$\tau_{1/2}$ ( $\text{min}^{-1}$ )
P-0	5	2.37	1.242	1.044	0.947	1.056
	10	2.44	3.573	1.136	0.514	1.946
	20	2.31	8.110	1.110	0.345	2.899
	40	2.37	25.82	1.085	0.218	4.587
P-5	5	2.22	1.001	1.000	0.893	1.120
	10	2.18	3.940	1.147	0.469	2.132
	20	2.04	9.382	1.118	0.285	3.509
	40	2.45	40.92	1.097	0.187	5.348
P-15	5	2.48	1.296	1.053	0.781	1.280
	10	2.33	3.713	1.140	0.502	1.992
	20	2.38	11.91	1.132	0.307	3.257
	40	2.36	40.51	1.097	0.171	5.848
P-25	5	2.34	1.720	1.115	0.703	1.422
	10	2.47	3.909	1.146	0.508	1.969
	20	2.63	14.28	1.142	0.313	3.915
	40	2.62	47.79	1.102	0.194	5.515

crystallization mechanism of PTFE and that the mode of the nucleation and growth in the primary crystallization stage may have been a one-dimensional homogeneous nucleation or a two-dimensional heterogeneous nucleation mechanism. Also, we found that all  $n$  values in the initial crystallization stage were close to 1. This revealed that a one-dimensional heterogeneous nucleation crystallization mechanism performed in the initial crystallization stage. Therefore, there were two crystallization stages in the crystallization process of PTFE. It is well known that  $Z_c$  and  $\tau_{1/2}$  values are used to compare the crystallization rate of samples under different conditions and that a higher  $Z_c$  or  $\tau_{1/2}$  indicates a faster crystallization rate. The data listed in Table II show that the values of  $Z_c$  (except for those of P-5 when  $\Phi$  was  $5^{\circ}\text{C}/\text{min}$ ) and  $\tau_{1/2}$  for each PTFE/SGM composite were larger than those of pure PTFE at a given  $\Phi$ . This indicated that the addition of SGMs accelerated the crystallization process of PTFE.

#### Ozawa method

Considering the effect of  $\Phi$  on the nonisothermal crystallization and on the basis of the assumption that the crystallization process was composed of infinite small isothermal crystallization steps, Ozawa<sup>16</sup> extended Avrami theory from isothermal crystallization to the nonisothermal case. The Ozawa equation is expressed as

$$\log\{-\ln[1 - X(t)]\} = \log K(T) + m \log \Phi \quad (6)$$

where  $K(T)$  is a function of  $\Phi$  and  $m$  is the Ozawa exponent, which is similar to  $n$ . Figure 5 illustrates the plots of  $\log\{-\ln[1 - X(t)]\}$  as a function of  $\log \Phi$  at various temperatures. If the Ozawa method was valid, the corresponding plots would have shown a

series of parallel straight lines. However, no straight line was obtained in Figure 5; thus, the Ozawa method failed to describe the nonisothermal crystallization process of both PTFE and the PTFE/SGM composites. According to researches reported by Shih et al.<sup>23</sup> and Ma et al.,<sup>24</sup> the failed description was attributed to an improper assumption, such as the neglect of secondary crystallization and trans-crystallization. However, Kostov et al.<sup>12</sup> testified that secondary crystallization was not observed in PTFE. Therefore, the reason may have been that the nonisothermal crystallization was a dynamic process in which the crystallization rate was no longer a constant but a function of time and  $\Phi$ ; thus, the quasi-isothermal treatment of the Ozawa model might be questionable.

#### Mo method

Another kinetic equation of nonisothermal crystallization proposed by Mo et al.<sup>20</sup> was derived from the combination of the Avrami equation [eq. (4)] with the Ozawa equation [eq. (6)] and is written as

$$\log \Phi = \log F(T) - \alpha \log t \quad (7)$$

where  $\alpha = n/m$ , or the ratio of the Avrami exponent to the Ozawa exponent, and  $F(T) = [K(T)/Z]^{1/m}$  is the value of  $\Phi$ , which has to be chosen within unit crystallization time to reach a defined  $X_c$  for the measured system. Plots of  $\log \Phi$  as a function of  $\log t$  at various  $X_c$  values are given in Figure 6. It was quite evident that these curves had good linearity and showed that the Mo method successfully described the nonisothermal crystallization process of PTFE and the PTFE/SGM composites.  $F(T)$  and  $\alpha$  calculated from the intercepts and slopes of the curves in Figure 6, along with

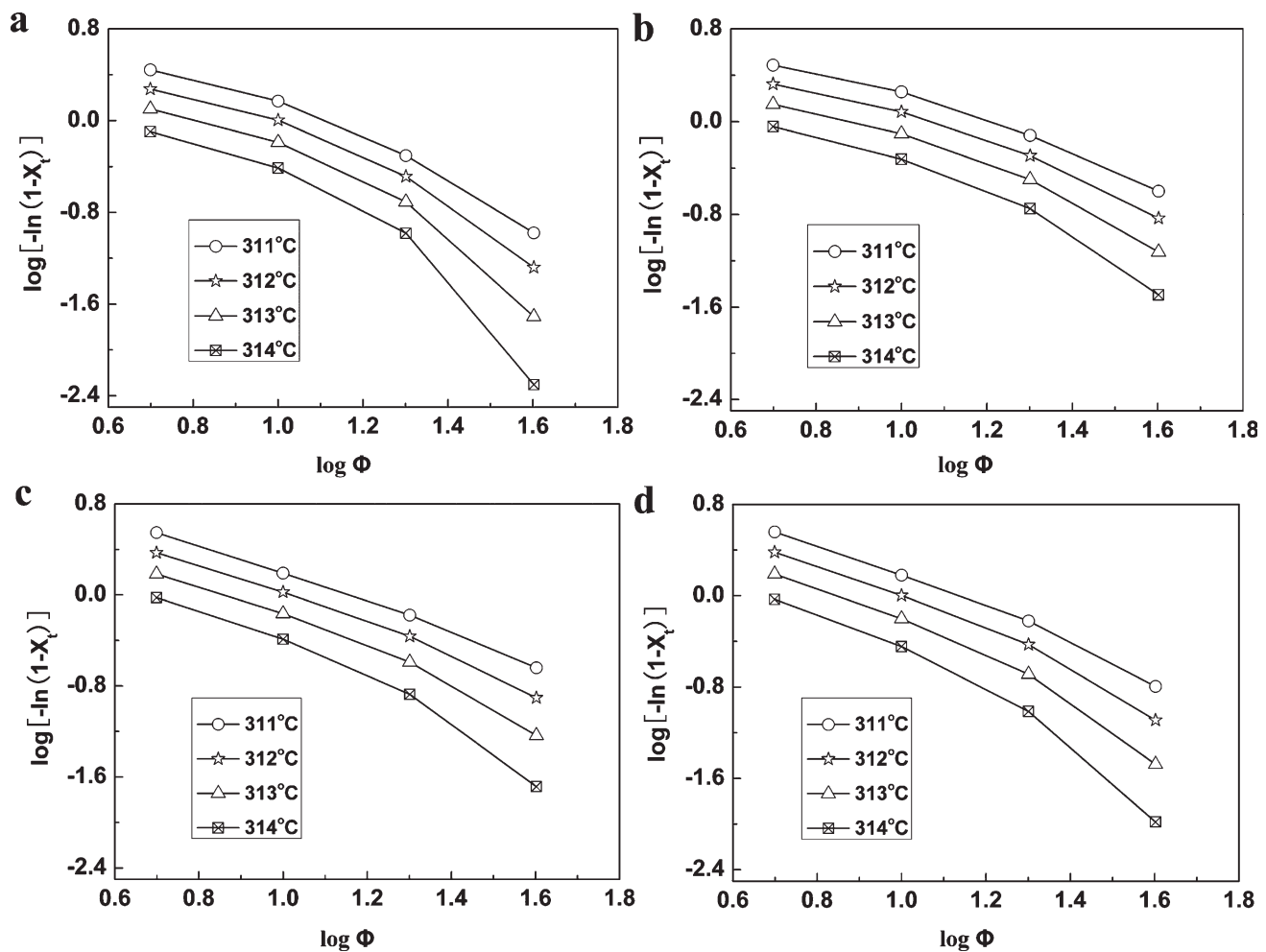


**Figure 5** Plots of  $\log[-\ln(1 - X_c)]$  versus  $\log \Phi$  at given temperatures for (a) P-0, (b) P-5, (c) P-15, and (d) P-25.

the corresponding correlation coefficients ( $r^2$ 's), are summarized in Table III. Obviously, the values of  $F(T)$  increased monotonously with increasing relative  $X_c$ , which meant that, within the unit crystallization time, a higher  $\Phi$  was required to obtain a higher  $X_c$ . However, no clear regularity was observed from the  $\alpha$  values. Furthermore, by comparing the  $F(T)$  values of different samples at the same relative  $X_c$ , we found that the values of P-5, P-15, and P-25 were lower than those of P-0. This suggested that each crystallization rate of the PTFE/SGM composites was higher than that of pure PTFE.

### $\Delta E$

$\Delta E$  was calculated by the Kissinger equation. The Kissinger equation can be expressed as follows:<sup>25</sup>

$$\frac{d(\ln \Phi / T_p^2)}{d(1/T_p)} = -\frac{\Delta E}{R} \quad (8)$$

where  $R$  is the universal gas constant. The  $\Delta E$  values of PTFE and the PTFE/SGM composites were determined from the slopes of the plots of  $\ln \Phi / T_p^2$  as a

function of  $1/T_p$ , and the results are listed in Table I. Apparently, the  $\Delta E$  value of PTFE was larger than that of each PTFE/SGM composite, which implied that the incorporation of SGM made crystallization easier. On the other hand, the  $\Delta E$  values of the PTFE/SGM composites increased monotonously from 232.1 to 283.5 kJ/mol with increasing content of SGM from 5 to 25%. We considered that SGM particles played two roles in the crystallization of the matrix. The SGM particles acted as a heterogeneous nucleating agent to facilitate crystallization at a relatively lower SGM content, whereas at a relatively higher content, the SGM particles acted as a physical hindrance to decrease the activity of the molecular segments and baffle the molecular segments to arrange into a crystal lattice. Therefore, the addition of SGM at an appropriate concentration was favorable to the crystallization of PTFE.

### CONCLUSIONS

Studies on the nonisothermal crystallization behavior of PTFE and PTFE/SGM composites were carried out

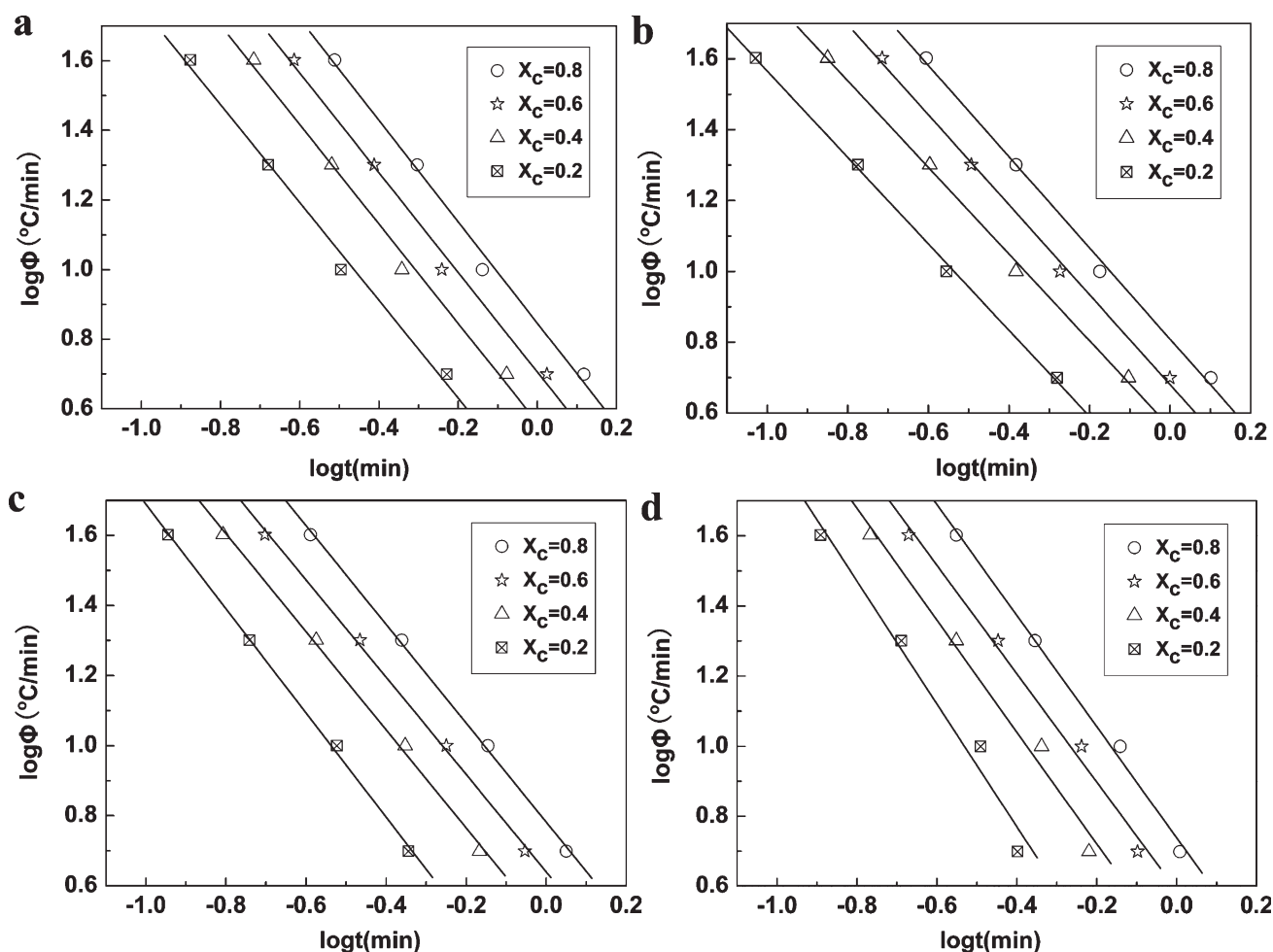


Figure 6 Plots of  $\log \Phi$  versus  $\log t$  at given relative  $X_c$  for (a) P-0, (b) P-5, (c) P-15, and (d) P-25.

with DSC at various  $\Phi$ 's. As  $\Phi$  increased, the exothermic peaks shifted to lower temperatures and  $X_c$  decreased. The crystallization behavior of the PTFE/

TABLE III  
Parameter Values of Nonisothermal Crystallization  
Obtained with the Mo Equation and the Corresponding  
 $r^2$  Values of PTFE and the PTFE/SGM Composites

No.	$X(t)$ (%)	$F(T)$	$\alpha$	$r^2$
P-0	20	2.24	1.41	0.9963
	40	3.63	1.42	0.9961
	60	5.07	1.43	0.9959
	80	7.01	1.45	0.9965
P-5	20	2.22	1.22	0.9992
	40	3.62	1.23	0.9988
	60	4.78	1.27	0.9985
	80	6.43	1.29	0.9981
P-15	20	1.59	1.48	0.9992
	40	3.05	1.40	0.9988
	60	4.37	1.39	0.9991
	80	6.05	1.41	0.9994
P-25	20	1.18	1.75	0.9875
	40	2.52	1.59	0.9920
	60	3.88	1.55	0.9949
	80	5.48	1.58	0.9976

SGM composites exhibited a much higher crystallization rate and a smaller  $t_{1/2}$  compared to the pure PTFE. The applicability of several kinetic methods for nonisothermal crystallization was examined. The Ozawa method failed to provide an adequate description of the crystallization data of PTFE and the PTFE/SGM composites. Both the Jeziorny and Mo methods successfully described the nonisothermal crystallization process of PTFE and the PTFE/SGM composites. The Jeziorny analysis indicated that the crystallization processes of PTFE and the PTFE/SGM composites were divided into initial and primary crystallization stages. The  $F(T)$  values obtained in the Mo analysis increased as the relative  $X_c$  increased. In addition, the activation energy for nonisothermal crystallization was evaluated with the Kissinger equation, and the  $\Delta E$  value decreased remarkably when a small amount of SGMs was added and then gradually increased with increasing SGM loading.

## References

1. Sperati, C. A.; Starkweather, H. W. *Fortschr Hochpolym Forsch* 1961, 2, 465.



2. Cox, J. M.; Wright, B. A.; Wright, W. W. *J Appl Polym Sci* 1964, 8, 2935.
3. Khedkar, J.; Negulescu, I.; Meletis, E. I. *Wear* 2002, 252, 361.
4. Xiang, D. H.; Tao, K. M. *J Appl Polym Sci* 2007, 103, 1035.
5. Lai, S. Q.; Yue, L.; Li, T. S. *J Appl Polym Sci* 2007, 106, 3091.
6. Gu, A. J.; Liang, G. Z.; Yuan, L. *Polym Adv Technol* 2008, 19, 1.
7. Bassett, D. C.; Davitt, R. *Polymer* 1974, 15, 721.
8. Ferry, L.; Vigier, G.; Vassoille, R.; Bessede, J. L. *Acta Polym* 1995, 46, 300.
9. Pucciariello, R.; Mancusi, C. *Ann NY Acad Sci* 1999, 879, 280.
10. Seo, Y. *Polym Eng Sci* 2000, 40, 1293.
11. Wang, X. Q.; Chen, D. R.; Han, J. C.; Du, S. Y. *J Appl Polym Sci* 2002, 83, 990.
12. Kostov, G.; Charadjiev, P.; Popov, A. *Eur Polym J* 1993, 29, 1025.
13. Liu, X. H.; Wu, Q. J.; Berglund, L. A.; Qi, Z. N. *Macromol Mater Eng* 2002, 287, 515.
14. Wunderlich, B. *Macromolecular Physics*; Academic: New York, 1976; Vol. 2.
15. Liu, T. X.; Mo, Z. S.; Zhang, H. F. *J Appl Polym Sci* 1998, 67, 815.
16. Ozawa, T. *Polymer* 1971, 12, 150.
17. Ziabicki, A. *Colloid Polym Sci* 1974, 252, 433.
18. Jeziorny, A. *Polymer* 1978, 19, 1142.
19. Gupta, A. K.; Purwar, S. T. *J Appl Polym Sci* 1984, 29, 1595.
20. Liu, J. P.; Mo, Z. S.; Qi, Y. C.; Zhang, H. F.; Chen, D. L. *Acta Polym Sinica* 1993, 1, 1.
21. Avrami, M. *J Chem Phys* 1939, 7, 1103.
22. Avrami, M. *J Chem Phys* 1940, 8, 212.
23. Shih, Y. F.; Wang, T. Y.; Jeng, R. J.; Wu, J. Y.; Wu, D. S. *J Appl Polym Sci* 2008, 110, 1068.
24. Ma, Y. L.; Hu, G. S.; Ren, X. L.; Wang, B. B. *Mater Sci Eng A* 2007, 460–461, 611.
25. Kissinger, H. E. *J Res Nat Bur Stand* 1956, 57, 217.